

**Title: A new model to quantify the probability of collision between birds and aircraft: applications for onboard lighting**

**Authors:**

- 1) Ryan B. Lunn<sup>1</sup>
- 2) Bradley F. Blackwell<sup>2</sup>
- 3) Esteban Fernández-Juricic<sup>1</sup>

<sup>1</sup> Department of Biological Sciences, Purdue University, 915 Mitch Daniels Blvd, West Lafayette, IN, 47907, United States of America

<sup>2</sup> United States Department of Agriculture, Animal and Plant Health and Inspection Services, National Wildlife Research Center, Sandusky, 610 Columbus Ave, OH, 44870, United States of America

**Corresponding Author:** Ryan B. Lunn, email: [rlunn@purdue.edu](mailto:rlunn@purdue.edu)

**Open Research Statement**

All code, files, and data generated from this study are available at <https://osf.io/zh68x/>

**Keywords:** Animal & Vehicle Collisions, Probability of Collision, Model, Escape Behavior, Bird & Aircraft Collisions, Canada Geese

## Abstract

Globally, bird and aircraft collisions are a major safety hazard and monetary expense for the aviation industry. Empirical evidence suggests that the behavioral response of the animal just prior to a collision is a critical factor in determining whether a collision occurs. However, no theoretical framework exists to predict the probability of a collision based on the escape response of the animal to an approaching vehicle. We adapted concepts from existing predator-prey theoretical frameworks to develop a novel model to quantify the outcome of an animal-vehicle interaction. Specifically, our model consists of two distinct phases. Phase one determines if a collision is even possible based on the amount of time the animal has available to clear the trajectory of the approaching vehicle. If the animal does not have enough time, then phase two of the model estimates the probability of collision based on the surface area of the vehicle given the location of the animal within the trajectory. We demonstrate the utility of the model by estimating the probability of collision between a Canada goose and an approaching Boeing-737 aircraft with the absence and presence of onboard lights of different wavelength, a technological intervention aimed at minimizing bird strikes. Our model predicts that when a Canada goose is within the trajectory of a Boeing-737, the average probability of collision is approximately 0.43; however, onboard lights with wavelengths tuned to the visual system of the species can reduce that probability on average by either 19% (red-light onboard) or 32% (blue-light onboard). The highest probability of collision occurred when the animal was in the center of the trajectory of the vehicle. The behaviors with the largest effect on reducing the probability of collision were an increase in flight-initiation distance and an increase in escape speed. Our approach provides a framework to quantitatively predict how the probability of collision might change across different species, vehicles, and situations, which could be used in forecasting the impacts of present and future transportation projects on wildlife populations.

## **Introduction**

Globally, collisions between birds and aircraft pose a major safety hazard and monetary expense for the aviation industry (Allan, 2000, Altringer et al., 2021, Dolbeer et al., 2023). As air traffic is slated to increase with the proliferation of unoccupied aerial systems (i.e., UAS) (Mulero-Pázmány et al., 2017, Federal Aviation Administration Aerospace Forecasts Fiscal Years 2024–2044, 2024, Davies et al., 2021), the frequency of bird and aircraft collisions, hereafter bird strikes, is expected to increase. At a time when bird populations are globally declining (Rosenberg et al. 2017, Burns et al. 2021, Lees et al. 2022), mitigating bird-strikes has the potential to reduce both avian and human mortality as well as economic damage.

We know from the empirical literature that animal behavioral responses to an imminent collision with an approaching vehicle are critical in determining whether a collision does (i.e., the two come into contact) or does not occur (i.e., near miss), hereafter referred to as the probability of collision (DeVault et al., 2015, Blackwell et al., 2019, Brieger et al., 2022). Mathematical models exist to predict whether a prey animal can escape an approaching predator based on properties of their escape response (Dill 1974, Domenici, 2002, Broom & Ruxton, 2005, Corcoran & Conner, 2016, Ruxton et al., 2018, Kawabata, et al., 2023, Bartashevich et al., 2024). However, these models have yet to be applied to quantify how changes in the behavioral response of an animal affect the probability of colliding with an approaching vehicle (DeVault et al. 2015, Guenin et al. 2024). Herein, we build upon existing models of predator-prey interactions to propose a novel model to estimate the probability of collision when an animal is exposed to an approaching vehicle.

Our study has three aims. First, we introduce a model that can be used to quantify the probability of collision considering variables such as escape trajectory, escape speed, vehicle size

and vehicle speed. The model also incorporates new elements such as the location of the animal within the trajectory of the vehicle, and a stochastic component based on estimates of the relative sizes of the vehicle and the animal. Second, we demonstrate the application of the probability of collision model to a scenario involving an approaching Boeing-737 aircraft and a Canada goose (*Branta canadensis*), a large bodied, abundant, flocking species that can cause substantial damage upon collision (Dolbeer et al. 2014, DeVault et al., 2018). We parameterized our model with empirical data found in the peer-reviewed literature of Canada goose escape responses to an approaching vehicle. Third, we then applied the model to a scenario where a Canada goose is approached by an aircraft but with onboard lights to investigate how different properties might affect the behavioral responses of Canada geese (Blackwell et al., 2012) and consequently the probability of collision.

Aircraft lighting of high chromatic contrast relative to the visual system of a target species has been proposed as a method to mitigate bird and aircraft collisions, especially beyond the airport boundary where mitigation methods are difficult to implement (Dolbeer et al., 2011, Blackwell & Fernández-Juricic, 2013). Specifically, experimental evidence has shown that these onboard lights tuned to the avian visual system increase the distance a bird first detects an approaching aircraft, ultimately allowing more time for the animal to execute an escape response (Blackwell et al., 2009, Blackwell et al., 2012, Doppler et al., 2015). Additional evidence suggests that lights might also facilitate a more effective escape response by promoting avoidance responses (Goller et al., 2018, Lunn et al., 2023). However, to date no quantitative estimates have been made for how changes in behavior caused by lights might reduce the probability of collision between a bird and an aircraft.

### *Probability of collision model overview*

Our model for the probability of collision has two distinct phases. Phase one calculates whether the animal has enough time to escape the trajectory of the approaching vehicle (Table 1). If the animal has enough time to escape the trajectory of the vehicle, then a collision is avoided. However, if the animal does not have enough time, then the vehicle overtakes the animal and therefore a collision is possible. Phase one assumes that the animal is within or near the trajectory of the vehicle and therefore a collision is possible, and that the trajectory of the vehicle is fixed (Table 2, Assumptions 1 & 2). Phase two assigns the animal some probability of collision depending on the location of the animal within the trajectory of the vehicle.

#### *Phase one*

Phase one rearranges the classic formula for speed (i.e.,  $Speed = \frac{Distance}{Time}$ ) and incorporates additional parameters to determine whether a collision is possible. Functionally, in phase one we estimate the time that the animal needs to escape the trajectory of the vehicle ( $T_a$ ) and the remaining amount of time until the vehicle reaches the location of the animal after escape is initiated ( $T_v$ ) (Table 1). If the time the animal needs to escape ( $T_a$ ) is great than or equal to the amount of time remaining prior to the vehicle reaching the animal ( $T_v$ ), then the situation results in a potential collision ( $T_a \geq T_v$ ). Alternatively, if the time the animal needs to escape ( $T_a$ ) is less than the time remaining prior to the arrival of the vehicle ( $T_v$ ), then a collision is avoided ( $T_a < T_v$ ). The time needed to escape the trajectory of the vehicle ( $T_a$ ) depends on the distance the animal needs to travel to safety ( $D_{min}$ ), the body length of the animal ( $l$ ), escape speed ( $S_a$ ), escape angle ( $\theta$ ), and sensory-motor delays as the animal reorients and begins to accelerate ( $\delta$ ) (Table 1, Fig.1). After initiating escape, the animal needs time to travel some minimum distance

to safety ( $D_{min}$ ) and additionally travel beyond its own body length ( $l$ ) to completely avoid a collision, where the maximum possible value of  $D_{min}$  is the entire width of the vehicle (Eq. 1).

$$D_{safe} = D_{min} + l \quad (\text{Eq.1})$$

$D_{safe}$  is the total distance the animal needs to travel to clear the trajectory of the vehicle.

Animals often combine a mixture of protean and optimal escape trajectories, alternatively escape angle ( $\theta$ ), to successfully escape or avoid an approaching threat, such as a natural predator (Domenici, 2002, Walker et al., 2005, Kimura & Kawabata, 2018, Kawabata et al., 2023). Escape angles ( $\theta$ ) are typically defined relative to the approach angle of the threat. Herein we define  $0^\circ$  as flight directly towards the approaching vehicle and  $180^\circ$  as flight directly away from the vehicle, where escape angles are limited between a range of  $0^\circ$  to  $180^\circ$ . Escape angles that differ from a perpendicular escape angle (i.e.,  $90^\circ$ ) extend the time needed for the animal to completely cross  $D_{safe}$ . Additionally,  $T_a$  is dependent upon the escape speed of the animal ( $S_a$ ) and the additional time required to reorient and accelerate as it enacts its escape response ( $\delta$ ) (Eq. 2; Figure 1).

$$T_a = \frac{D_{safe}}{S_a \sin(\theta)} + \delta \quad (\text{Eq.2})$$

Equation 2 assumes a constant escape speed by the animal (Table 2, Assumption 3).

The time remaining until the vehicle reaches the location of the animal after escape initiation ( $T_v$ ) depends on the flight-initiation distance ( $D_{FID}$ ), escape speed ( $S_a$ ), and escape angle ( $\theta$ ) of the animal, and the approach speed of the vehicle ( $S_v$ ) (Table 1, Fig.1). After the animal initiates its escape response ( $D_{FID}$ ), it has a limited amount before the vehicle reaches the location of the animal depending on the approach speed of the vehicle ( $S_v$ ). However, depending on the escape speed ( $S_a$ ) and angle ( $\theta$ ) of the animal, the vehicle will reach the position of the

animal either relatively sooner or later as the animal moves either farther away or closer to the approaching vehicle (Eq. 3).

$$T_v = \frac{D_{FID}}{S_v + (\cos(\theta) * S_a)} \quad (\text{Eq.3})$$

Equation 3 assumes a constant vehicle approach speed ( $S_v$ ) and animal escape speed ( $S_a$ ).

Consequently, if  $T_a$  (i.e., time needed to escape) is greater than or equal to  $T_v$  (i.e., time remaining to successfully escape), a collision is possible. If a collision is possible then phase two of the model estimates some probability of collision based on the location of the animal within the trajectory of the vehicle. However, phase two is not applicable to situations where  $T_a < T_v$  because a collision is entirely avoided, assuming the animal does not change directions or stop (Table 2, Assumption 3).

#### *Phase two*

Phase two has two distinct components: 1) an estimate of the location of the animal within the trajectory of the vehicle at the moment of collision ( $D_{\text{collision}}$ ); and 2) the assignment of the probability of collision based on that location (i.e.,  $P(\text{Collision})$ ).

We estimated  $D_{\text{collision}}$  based on the absolute minimum distance to safety ( $D_{\text{min}}$ ), the entirety of the vehicles width ( $D_{\text{width}}$ ), the escape speed ( $S_a$ ) and angle ( $\theta$ ) of the animal, and the duration of time that elapsed since the animal initiated escape ( $T_v$ ). First, the minimum distance to safety ( $D_{\text{min}}$ ) and the trajectory width of the vehicle ( $D_{\text{width}}$ ) are used to estimate the initial position of the animal in the trajectory of the vehicle at the time when escape is initiated ( $D_{\text{initial}}$ ) (Table 1, Fig.1, Eq. 4).

$$D_{\text{initial}} = D_{\text{min}} - D_{\text{width}} \quad (\text{Eq.4})$$

From the initial location of the animal  $D_{\text{initial}}$  the model estimates how much further the animal

travels within the trajectory of the vehicle while the vehicle continues to approach by multiplying escape speed ( $S_a$ ), angle ( $\theta$ ), and the time remaining since escape initiation ( $T_v$ , see Eq.3), which yields equation 5.

$$D_{collision} = D_{initial} + (\cos(\theta) * S_a * T_v) \quad (\text{Eq. 5})$$

$D_{collision}$  is the location, specifically the midpoint, of the animal in the trajectory of the vehicle at the moment the vehicle reaches the animal.

Estimates of  $P(\text{Collision})$  are based on the frontal surface area of the vehicle ( $A_{front}$ ) and width of the animal the point of contact based on the location of the animal in the trajectory of the vehicle ( $D_{collision}$ ) and body length of the animal ( $l$ ) (Table 1). We defined the trajectory of the vehicle as a 2-D planar space bound by vehicle width ( $D_{width}$ ) and height ( $D_{height}$ ), which, respectively, can be thought of as the x and y axes (Fig. 2). We estimated the probability of collision as the ratio between all the space occupied by the frontal surface area of the vehicle ( $A_{front}$ ) and the entire surface area at that location on the x-axis where the animal could be (i.e., product of  $l$  and  $D_{height}$ ), assuming the animal (i.e., a bird) could be at any random altitude (i.e., y-axis) within the collision window (Table 2, Assumption 4, Eq.6a-6c).

$$coord_1 = D_{collision} - (\frac{l}{2}) \quad (\text{Eq. 6a})$$

$$coord_2 = D_{collision} + (\frac{l}{2}) \quad (\text{Eq. 6b})$$

$$P(\text{Collision}) = \frac{1}{D_{height} * l} \int_{coord_1}^{coord_2} A_{front} \quad (\text{Eq. 6c})$$

## **Methods**

### *Parameter selection & simulation approach*

We applied our model to estimate the probability of collision for a scenario where a high-speed aircraft (i.e., a Boeing737) approaches a Canada goose. We investigated how the probability of



collision changes by systematically iterating through a range of realistic values for four different parameters: goose escape speed ( $S_a$ ), sensory-motor delay ( $\delta$ ), the minimum distance to safety ( $D_{\min}$ ), and aircraft approach speed ( $S_v$ ). (Table 1). Herein, we used only a single value for body length ( $l$ ), where we defined body length as the linear distance from the tip of the beak to the outer edges of the tail feathers (115 cm, Bellrose, 1976).

We varied escape speed ( $S_a$ ) between 1 m/s to 17 m/s, in increments of 2 m/s, based on the recorded flight speed of Canada geese (Wege & Raveling, 1984). The sensory-motor delay values ( $\delta$ ) varied between 0 to 1 second in increments of 0.1 secs based on the observed response delays of different bird species (Provini et al., 2012, Guenin et al., 2024). A sensory-motor delay of 0 seconds represents a scenario where the animal is actively moving when it crosses into the trajectory of the vehicle, whereas 1 second means the animal took an entire second before it actually began to move. The minimum distance to safety ( $D_{\min}$ ) varied from 1 to 14.35 m by increments of 1.48 m for a total of 10 different intervals. We chose 14.35 m as the maximum distance to safety based on the width between the edges of the horizontal stabilizers of a 737 commercial aircraft (Fig. 2). We elected not to use the entire width of the aircraft wingspan because the collisions with the highest probability of damage, once a collision occurs, are impacts to the fuselage or engine ingestion (Liu et al., 2018, Dolbeer et al., 2023) (Fig. 2). Lastly, we varied aircraft approach speed ( $S_v$ ) between 70.47 (i.e., 150 knots) to 270.97 m/s by increments of 14.32 m/s for a total of 15 different approach speeds based on the range of Federal Aviation Administration recommended approach speeds that occur at different flight phases (e.g., take-off run, climb, cruise, approach, landing) (Instrument Procedures Handbook: FAA-H-8083-16A, 2017).

For each run of the model, we simulated a single flight-initiation distance ( $D_{FID}$ ) and

escape angle ( $\theta$ ). We simulated flight-initiation distance values ( $D_{FID}$ ) from a normal distribution with a mean of 56.2 m and a standard deviation of 16.5 m, based on Canada goose escape responses to direct approaches by an automobile (i.e., a truck) (Blackwell et al. 2019). Escape angle values ( $\theta$ ) were simulated from one of two different uniform distributions. Birds either received an escape angle ( $\theta$ ) from a uniform distribution with escape angles ( $\theta$ ) ranging from 0.01 to 89.99°, hereafter referred to as the “toward” distribution, or from a uniform distribution with escape angles ( $\theta$ ) ranging from 90.01 to 179.99°, hereafter the “away” distribution. In our parametrization of the model, geese had a different probability of receiving either an escape angle from the “toward” (0.58) or “away” (0.42) distribution based on the frequency of different Canada goose behavioral responses reported by pilots obtained from the “Remarks” section of the Federal Aviation Administration wildlife collision database (Appendix S1).

To account for variation in model predictions attributable to differences in simulated flight-initiation distance ( $D_{FID}$ ) and escape angle ( $\theta$ ) values, we ran the model with 500 iterations for each unique combination of parameter values.

### *Estimating the probability of collision*

We quantified the probability of collision by digitizing a to-scale-schematic of a Boeing-737 (Fig. 2). We estimated the frontal surface area of the vehicle ( $A_{front}$ ) by summing all the pixels occupied by the aircraft (Fig. 2), divided by the total number of pixels within a specific subsection along the x-axis defined by the length of the goose and height of the aircraft, hereafter referred to as the “collision window”. We converted the length of the goose to pixels by first dividing the width of the trajectory (i. e., 14.35 m) by the width of the aircraft schematic image

(i.e., 1031 pixels) (Fig. 2) to estimate the m/pixels conversion factor (0.0139 m/pixels), then divided goose length ( $l$ ) (i.e., 115 cm) by the conversion factor to estimate the length of a goose in nearest whole pixels (83 pixels).

#### *Model application*

We applied our model to quantify how lights of different wavelengths onboard an approaching aircraft might affect the probability of collision through altering the behavior of Canada geese. Lights have been shown to lead to earlier alert responses to approaching vehicles (Blackwell et al., 2012). Specifically, Canada geese alerted 4.1 seconds earlier to an approaching aircraft with a light turned on ( $11.4 \pm 4.4$  sec) relative to an aircraft with a light turned off ( $7.3 \pm 4.4$ ) (Blackwell et al., 2012). This early alert provides an opportunity for the animal to escape sooner, thus expanding the range of potential flight-initiation distances ( $D_{FID}$ ) (Blackwell & Fernández-Juricic, 2013). Consequently, for an aircraft approaching with lights on we simulated flight-initiation distance ( $D_{FID}$ ) values from a uniform distribution with a minimum of 0 m and maximum flight-initiation distance ( $D_{FID}$ ) based on the maximum possible alert distance. We estimated the maximum possible alert distance by multiplying the temporal benefit provided by the light source, hereafter  $\beta$ , by the aircrafts approach speed. We systematically varied the temporal benefit of the light source ( $\beta$ ) from 0 to 8.5 seconds by increments of 0.88 seconds for 10 different intervals, based on the mean observed temporal benefit (4.1 sec) and SD in alert time (4.4 sec) observed in Blackwell et al. (2012).

Light wavelengths of high chromatic contrast have also been shown to affect the avoidance responses in Canada geese in a single choice experiment (i.e., a T-maze test), where differences in the probability of avoidance could potentially translate to differences in the escape

angle of the animal (Lunn et al., 2023). Lunn et al., 2023 found that after repeated exposures geese tended to avoid a 483 nm light (i.e., blue) (probability of avoidance 0.65) and were attracted to 631 nm light (i.e., red) (probability of avoidance 0.11). Consequently, we explored how the probability of collision changes for different wavelengths of high chromatic contrast (i.e., a blue- and red-light) assuming an avoidance response translates to an escape trajectory away from the approaching aircraft (i.e., an escape angle ( $\theta$ )  $> 90$  deg). Specifically, in a blue-light scenario geese had a 65% chance of receiving an escape angle from the “away” distribution, where in a red-light scenario geese had a 11% chance of receiving an escape angle from the “away” distribution according to the difference in the probability of avoidance reported in the final trials of Lunn et al. 2023.

No study that we are aware of has examined how different wavelengths of light simultaneously affect different combinations of flight-initiation distance ( $D_{FID}$ ) and escape angles ( $\theta$ ). Lunn’s et al. (2023) findings indicate that geese developed an attraction response to the red-light but showed a mild avoidance response to the blue-light after repeated exposures. We assumed for both the blue- and red-light scenarios that “toward” escape angles are indicative of a potential attraction response to the lights (not necessarily to the approaching aircraft) and thus paired them with shorter flight-initiation distances ( $D_{FID}$ ); whereas “away” escape angles were indicative of avoidance and paired with longer flight-initiation distances ( $D_{FID}$ ). Specifically, the presence of attractants such as a food source, potential mate, or flock members results in shorter flight-initiation distances, where the presences of an aversive stimuli or repellent associated with greater perceived risk, such as faster and more direct predator approaches, results in longer flight-initiation distances (Ydenberg & Dill 1986, Cooper et al., 2009, Blackwell et al. 2019, Ventura et al., 2021, Hammer et al., 2025). Additionally, birds can

either be attracted or repelled by different light stimuli (Poot et al., 2008, Rodríguez et al., 2017, Adams et al., 2021, Van Doren et al., 2021), potentially leading either to shorter or longer flight-initiation distances, respectively.

For both the blue- and red-light scenarios if the simulated escape angle ( $\theta$ ) was received from the “toward” distribution then consequently the flight-initiation distance ( $D_{FID}$ ) was simulated from the same distribution as a no-light scenario (i.e., normal distribution, mean= 56.2 m, SD=16.5, and not affected by  $\beta$ ). However, if an escape angle ( $\theta$ ) was received from the “away” distribution, then consequently flight-initiation distance values were simulated from the distribution affected by  $\beta$  (i.e., a uniform distribution ranging from 0, to  $S_a \times \beta$ ).

### *Reporting results*

We generated a total of 222,750,000 predictions of whether a collision would or would not occur with our model for all combinations of goose escape speed ( $S_a$ ), sensory-motor delays ( $\delta$ ), the minimum distance to safety ( $D_{min}$ ), aircraft approach speed ( $S_v$ ), and the three different light scenarios (i.e., no-light, blue-light, red-light) which included the temporal benefit ( $\beta$ ) afforded by a light onboard. For each combination of parameters, we generated 500 predictions with different simulated values for flight-initiation distance ( $D_{FID}$ ) and escape angle ( $\theta$ ).

We present the model predictions for the probability of collision in Figures 3 and 4, where both figures show the relationship between the probability of collision and a single variable. In Figure 3, the x-axes were variables that we systematically manipulated, whereas in Figure 4 the x-axes are simulated variables (see above). We estimated the predicted probability of collision in Figure 3 by first summing the number of collisions that occurred for each unique combination of parameters and then divided the total by 500, representing the number of

different runs of the model with simulated flight-initiation distance ( $D_{FID}$ ) and escape angle ( $\theta$ ) values. We estimated the predicted probability of collision in Figure 4 by first binning both flight-initiation distance ( $D_{FID}$ ) and escape angle ( $\theta$ ) to within 0.1 of either a meter or degree and then added the total number of collisions that occurred within that bin divided by the total number of predictions within that bin. To describe the relationship between our continuous variables and the probability of collision regarding the three different light scenarios, we fitted a curve from a general additive model using the *geom\_smooth* in the *ggplot2* package (Wickham & Chang, 2016). The results of each figure can be interpreted as the average effect of that single parameter value on the probability of collision across all other possible parameter values.

## **Results**

### *Overview*

First, the mean probability of collision among all combinations of parameters was the lowest for the blue-light scenario (mean  $\pm$  SD,  $0.292 \pm 0.167$ ), with an increase for the red-light scenario ( $0.347 \pm 0.161$ ), and with the highest probability of collision occurring for the no-light scenario ( $0.429 \pm 0.189$ ) (Fig. 3a). Second, an increase in escape speed of the animal ( $S_a$ ) generally resulted in a non-linear asymptotic decrease in the probability of collision (Fig. 3b.). For the blue- and red-light scenarios, probability of collision decreased at a decreasing rate with escape speed. In contrast, the no-light scenario yielded a probability of collision that decreased but at an increasing rate with increasing escape speed (Fig. 3b). As sensory-motor delays increased, the probability of collision increased linearly and slightly, with a similar pattern across all three light scenarios (Fig. 3c). An increase in aircraft approach speed resulted in the probability of collision increasing to an asymptote for each light scenario (no-light > red-light > blue-light; Fig. 3d). The

relationship between the minimum distance to safety and the probability of collision was multimodal with three different inflection points (Fig. 3e). Generally, as the minimum distance to safety increased, so did the probability of collision. However, the shape of the curve strongly reflected the difference in the probability of collision based on the shape of the aircraft and the location of the animal within the trajectory. Specifically, the probability of collision was highest when the location of the animal within the trajectory of the aircraft coincided with either the fuselage or the engines, where this pattern was similar for all three light scenarios (Fig. 3e). Also, as the temporal benefit afforded by a light source increased, the probability of collision decreased to an asymptote and was only relevant for the blue- and red-light scenarios (Fig. 3f).

Larger flight-initiation distances ( $D_{FID}$ ) resulted in dramatically lower probabilities of collision for both the blue- and red-light scenarios (Fig 4a). Additionally, escape angles ( $\theta$ ) closer to  $90^\circ$  (i.e., escaping perpendicularly to the approaching vehicle) had a lower probability of collision relative to escape angles ( $\theta$ ) closer to either  $0^\circ$  or  $180^\circ$  (Fig. 4b). The “away” escape angles for both the blue- and red-light scenarios (i.e., paired with longer flight-initiation distance ( $D_{FID}$ )) yielded a dramatically lower probability of collision, in contrast to a perpendicular escape angle (Fig. 4b).

## **Discussion**

To summarize, we built upon an existing theoretical foundation (Domenici, 2002, Kawabata, et al., 2023) to propose a new mathematical model to estimate the probability of collision an animal faces given it is within the trajectory of vehicle, where herein applied to an approaching aircraft. Our model quantifies how differences in specific aspects of an escape response in the final seconds prior to the arrival of a high-speed approaching vehicle affects the probability of

collision. We then applied the model to quantify how a given technological intervention (i.e., onboard light stimuli) aimed at altering the escape response of the animal subsequently affects the probability of collision. Our model demonstrates the importance of considering how animals simultaneously alter multiple properties of an escape response to reduce the probability of collision, how the probability of collision varies depending on the location of the animal within the trajectory of the vehicle, and that the presence of onboard lighting tuned to eyes of the target species has the potential to reduce the probability of collision.

Animals often rely on a combination of several different sequential behaviors to reduce the mortality risk associated with an approaching predator (Evans et al., 2019, Branco & Redgrave, 2020). Evidence suggests that animals rely on similar behaviors when attempting to avoid approaching vehicles (Lima et al., 2015, DeVault et al., 2015, Lunn et al., 2022). Specifically, individuals can adjust their flight-initiation distance (Ydenberg & Dill 1986, Stankowich & Blumstein, 2005, Cooper & Blumstein, 2015), escape speed (Domenici & Blake, 1991, Lind et al., 2002), escape angle (Domenici & Blake, 1993, Domenici et al., 2011a, Domenici et al., 2011b), or opt to not escape at all (Broom & Ruxton, 2005, Cooper 2009b), Blackwell et al., 2020), to reduce mortality risk from an approaching threat (Caro et al., 2005).

The model can be used to identify the components of an escape response that have the largest effect on the probability of collision. Technological interventions or management can then target these specific behaviors of relatively larger effect size to enact the larger reductions in the probability of collision. For instance, in the case of Canada geese and an approaching 737 with no-light onboard, flight-initiation distance had the largest effect, where an increase from 0 m (0.460) to greater than 120 m (0.361) resulted in a 21.6 % decrease in the probability of collision (Fig. 4a). Differences in escape speed had the second largest effect, where an increase



from 0 (0.467) to 17 m/s (0.377) resulted in a 19.3% decrease in the probability of collision (Fig. 3b). Lastly, difference in escape angle from 0° (0.467) or 180° (0.464) to 90° (0.397) (Fig. 4b) respectively resulted in a 14.9% and 14.4% decrease in the probability of collision, respectively (Fig. 3c). Thus, we would expect that a strategy aimed at increasing Canada goose flight-initiation distance or escape speed would yield the largest reduction in the probability of collision relative to an approaching 737.

Our model also enables us to quantify how different vehicle approach scenarios affect the probability of collision, which can aid in developing collision mitigation strategies. For example, in the case of a 737 approaching a Canada goose, the location of the animal in the trajectory of the vehicle had the largest effect, where the difference between a minimum distance to safety of 1 m (0.102) versus 8.42 m (0.673) resulted in a 570% increase in the probability of collision. Specifically, the three inflection points (i.e., peaks) in Figure 3e correspond to the aircraft engines and fuselage, where the probability of collision increases due to their larger frontal surface areas. The predictions of our model align with the Federal Aviation Administration's wildlife strike database, where the most frequently struck locations of Canada geese on a 737 are the engines and the fuselage (n=193, Federal Aviation Administration Wildlife Strike Database) (Fig. 5a & b). A potential mitigation strategy therefore might focus on deterring birds away from sections of the aircraft with the largest frontal surface area.

Our model also provides a quantitative framework to make predictions about high-speed vehicle approach scenarios that are difficult to test empirically. Previously the fastest simulated approach speed empirically tested was 100 m/s by DeVault et al., 2015 (Fig. 5c). In our example with a Canada goose and a Boeing-737, we were able to estimate that the probability of collision increased by 27% from 70 (0.359) to 271 (0.457) m/s, extremely fast approach speeds.

371 Additionally, previous empirical studies have been limited to estimating whether a collision  
372 occurs based on only a few properties of an escape response (i.e., flight-initiation distance) and  
373 approaching vehicle (i.e., approach speed, vehicle width) (DeVault et al. 2015, Guenin et al.,  
374 2024). Our model proposes a framework for the additional variables that need to be collected to  
375 more accurately predict the outcome of an animal-vehicle interaction. While the predictions of  
376 our model align qualitatively with the empirical data (i.e., an increase in approach is associated  
377 with an increase in the probability of collision; DeVault et al., 2015, Guenin et al., 2024), the  
378 disparity in the probability of collision estimates between empirical and theoretical approaches  
379 (Fig. 5c) is likely due to our model considering how animals might alter many different  
380 components of their escape response simultaneously.

381 Both the probability of capture in the context of predator-prey interactions and the  
382 probability of collision in the context of animal-vehicle interactions rely on similar variables to  
383 quantify the outcome of an interaction with either a predator or a vehicle; however, additional  
384 assumptions and parameters are needed to estimate the probability of collision (Table 2). We  
385 argue that three major differences need to be considered. First, the probability of collision,  
386 especially for larger vehicles, is often not homogenous throughout trajectory of the vehicle (i.e.,  
387 portions with larger frontal surface area increase the probability of collision). As a result, the  
388 specific location of the animal within that trajectory should be considered, because a collision  
389 still might be avoided despite the vehicle reaching the location of the animal (e.g., a goose  
390 passing over the fuselage of the aircraft, see Phase two above).

391 Second, vehicles generally remain on a fixed and linear trajectory when approaching an  
392 animal as opposed to the dynamic trajectories of predators (Peterson et al., 2021). Models of  
393 predator-prey capture vary in whether they assume a predator approaches linearly or non-linearly

(Corcoran & Conner, 2016, Domenici, 2002, Kawabata et al., 2023). Vehicles are commonly limited to travelling on a designated substrate (i.e., road) or predetermined course (i.e., flight path), especially at faster speeds; therefore, when modeling animal vehicle collisions generally a linear approach can be assumed. Yet, a fixed and linear trajectory does not necessarily mean that the behavior of the vehicle does not change (e.g., pilots alter flight paths, speeds, etc.). An important component for future research is to assess the effects of driver behavior seconds prior to a collision (e.g., Pakula et al., 2023).

Third, the probability of collision is dependent on the approach angle of the vehicle. In empirical studies, approach angles are often categorized as either direct or indirect, defined by whether the trajectory of the predator intersects or simply bypasses the prey animal (e.g., Domenici, 2002, Stankowich & Blumstein 2005). However, the threshold approach angle that distinguishes between direct versus indirect angles is generally not explicitly defined, primarily because predators can dynamically alter their approach angle based on prey escape trajectories as they get closer (Howland, 1974, Corcoran & Conner, 2016, Peterson et al., 2021).

However, because vehicles are often limited to fixed trajectories (see above), we propose that the critical angle of a direct or indirect approach can be quantitatively defined as:

$$\theta_{threshold} = \sin^{-1} \left( \frac{D_{half} + l}{D_{mid}} \right); \quad (\text{Eq. 7})$$

where  $\theta_{threshold}$  is the critical approach angle differentiating between an indirect and direct approach,  $D_{mid}$  is the distance between the center of the vehicle and the animal, and  $D_{half}$  is half the maximum width of the vehicle, and  $l$  is the length of the animal. Specifically, vehicle approach angles greater than  $\theta_{threshold}$  will equate to an indirect approach where if the animal does not enact an escape response a collision can be avoided, where approach angles less than or equal  $\theta_{threshold}$  will result in a potential collision if no response is enacted. The probability of

collision with a vehicle being completely dependent on approach angle might explain in part why some animals appear to adopt relatively shorter flight-initiation distances (Holmes et al., 1993, Blackwell et al., 2020), not flee at all (Guenin et al., 2024), or flee after the vehicle has passed (Pfeiffer et al., 2025) because the probability of collision is 0 for an indirect approach.

Importantly, equation 7 does not explicitly affect the predictions of our model because assumption 1 (Table 2) states the vehicle is approaching directly and therefore the approach angle is below  $\theta_{threshold}$  and a collision is possible, if no response is enacted. As computer vision technology becomes further integrated into automated vehicle navigation (i.e., advanced air mobility) estimating the vehicles approach angle ( $\theta_{threshold}$ ) relative to a detected wildlife hazard could be important in monitoring the prevailing probability of collision and whether collision avoidance measures are necessary by the vehicle (Huijser et al., 2015, Corcoran et al., 2021, Nandutu et al., 2022).

The Federal Aviation Administration's wildlife strike database reports that interactions with Canada geese and aircraft over a 23-year period have cost the airline industry approximately 183 million dollars, a 7.95-million-dollar annual cost (Dolbeer et al., 2023). Our model suggests that blue and red onboard lighting tuned to the eyes of Canada geese would reduce the probability of collision by about 14 % and 8%, respectively, which potentially could have saved 25 and 15 million US dollars, respectively, over a 23-year period for just one species. However, a more structured analysis is necessary to truly estimate the potential financial savings and variation in savings afforded by light stimuli following the approaches put forth by Altringer et al. (2021, 2024). Additionally, these estimates are based on assumptions about how animals change multiple aspects of their escape behavior simultaneously in response to a light stimulus, and future research needs to evaluate these assumptions.

Future efforts to quantify the probability of collision for an approaching vehicle can build upon this existing model in several concrete ways. First, our modelling approach can be applied to other vehicle types (e.g., rotorcraft, automobiles, boats, etc.) and other taxa of management or conservation concerns. Second, in our modelling approach we did not incorporate any parameter or make any assumption about how animals delay escape after detection and continue to assess an approaching threat before initiating escape (Blumstein 2010, Chan et al., 2010, DeVault et al., 2015, Lunn et al., 2022, Guenin et al., 2024). As such, the absolute value for the probability of collision estimates are most likely conservative (i.e., smaller), especially given the extremely fast range of speeds we used to model an approaching aircraft. Future studies quantifying the probability of collision should explicitly incorporate a delay in time for risk assessment after detection and before flight-initiation distance into estimates of the time needed for the animal to clear the path trajectory of the vehicle. Third, our model implicitly assumes that the altitude of the animal in the path trajectory of the vehicle is random because the animal could be at potentially at any height (Fig. 2). In reality, the aircraft could be ascending or descending, and the bird as well could be attempting to gain or lose altitude to escape the trajectory of the vehicle. We did not assume any specific height within the trajectory of the vehicle because of the scarcity of empirical data to support a given range. However, if we had data on both take-off velocity and take-off or dive angle for Canada geese, we could improve the accuracy of the probability of collision estimates.

We envision that our model be applied to quantitatively estimate the probability of collision for various species and different vehicle approach scenarios, which could ultimately aid in forecasting the impacts of present and future transportation projects on wildlife populations. Additionally, our model allows us to estimate the probability of specific components of the

aircraft (fuselage, engines, wings, etc.) being struck, helping in the estimation of economic damage and safety hazards (Dolbeer et al., 2023). Overall, our framework can be used to develop targeted and preventative animal vehicle collision mitigation strategies, especially as air-traffic volume is forecasted to increase.

482  
483  
484  
485  
486  
487  
488  
489  
490  
491  
492  
493  
494  
495  
496  
497  
498  
499  
500  
501  
502  
503  
504  
505  
506  
507

**Acknowledgements:**

Our work was funded *via* the Cooperative Agreement with the U.S. Department of Agriculture, Animal and Plant Health Inspection Service, Wildlife Services (WS), National Wildlife Research Center (FAIN: AP22WSNWRC00C006), and based on funding received by WS *via* the Interagency Agreement with the U.S. Federal Aviation Administration (FAA Interagency No. 692M15-19-T-00017). Findings reported herein do not necessarily reflect the policy of the FAA or the USDA.

**Author Contributions:**

- Ryan B. Lunn: Conceptualization, Methodology, Data processing & analysis, Visualization, Writing-original draft, writing-review and editing, project administration
- Bradley F. Blackwell: Funding acquisition, Conceptualization, Writing-original draft, Writing-review and editing, Project Administration
- Esteban Fernández-Juricic: Funding Acquisition, Conceptualization, Methodology, Data processing & analysis, Writing-original draft, Writing-review and editing, Project Administration

**Conflict of Interest:**

No conflict of interest declared

## References

1. Adams, Carrie Ann, Esteban Fernández-Juricic, Erin Michael Bayne, and Colleen Cassady St. Clair. 2021. "Effects of artificial light on bird movement and distribution: a systematic map." *Environmental Evidence* 10, no. 1: 37. <https://doi.org/10.1186/s13750-021-00246-8>
2. Allan, John. R. 2000. "The costs of bird strikes and bird strike prevention". *Human conflicts with wildlife: economic considerations*, 18.
3. Altringer, Levi, Michael J. Begier, Jenny E. Washburn, and Stephanie A. Shwiff. 2024. "Estimating the impact of airport wildlife hazards management on realized wildlife strike risk." *Scientific Reports* 14, no. 1: 29018. <https://doi.org/10.1038/s41598-024-79946-3>
4. Altringer, Levi, Jordan Navin, Michael J. Begier, Stephanie A. Shwiff, and Aaron Anderson. 2021. "Estimating wildlife strike costs at US airports: A machine learning approach." *Transportation Research Part D: Transport and Environment* 97. <https://doi.org/10.1016/j.trd.2021.102907>.
5. Bartashevich, Palina, James E. Herbert-Read, Matthew J. Hansen, Félicie Dhellemmes, Paolo Domenici, Jens Krause, and Pawel Romanczuk. 2024. "Collective anti-predator escape manoeuvres through optimal attack and avoidance strategies." *Communications Biology* 7, no. 1: 1586. <https://doi.org/10.1038/s42003-024-07267-2>.
6. Bellrose, Frank Chapman. 1976. *Ducks, geese and swans of North America*. Harrisburg. Stackpole Books.



7. Blackwell, Bradley F., Travis L. DeVault, Thomas W. Seamans, Steven L. Lima, Patrice Baumhardt, and Esteban Fernández-Juricic. 2012. "Exploiting avian vision with aircraft lighting to reduce bird strikes." *Journal of Applied Ecology* 49, no. 4: 758-766. <https://doi.org/10.1111/j.1365-2664.2012.02165.x>
8. Blackwell, Bradley F., and Esteban Fernández-Juricic. 2013. "Behavior and physiology in the development and application of visual deterrents at airports." *In Wildlife in airport environments: preventing animal–aircraft collisions through science-based management*, pp. 11–22, 1st edn. Baltimore, MD: Johns Hopkins University Press.
9. Blackwell, Bradley F., Esteban Fernandez-Juricic, Thomas W. Seamans, and Tracy Dolan. 2009. "Avian visual system configuration and behavioural response to object approach." *Animal Behaviour* 77, no. 3: 673-684. <https://doi.org/10.1016/j.anbehav.2008.11.017>
10. Blackwell, Bradley F., Thomas W. Seamans, Travis L. DeVault, Steven L. Lima, Morgan B. Pfeiffer, and Esteban Fernández-Juricic. 2019. "Social information affects Canada goose alert and escape responses to vehicle approach: implications for animal–vehicle collisions." *PeerJ* 7:e8164. <https://doi.org/10.7717/peerj.8164>.
11. Blackwell, Bradley F., Thomas W. Seamans, Travis L. DeVault, Randy J. Outward, and Esteban Fernández-Juricic. 2020. "American kestrel responses to aircraft in an airport environment." *Journal of Raptor Research* 54, no. 3: 295-302. <https://doi.org/10.3356/0892-1016-54.3.295>

12. Blumstein, Daniel T. "Flush early and avoid the rush: a general rule of antipredator behavior?." *Behavioral Ecology* 21, no. 3 (2010): 440-442.  
<https://doi.org/10.1093/beheco/arq030>
13. Branco, Tiago, and Peter Redgrave. 2020. "The neural basis of escape behavior in vertebrates." *Annual review of neuroscience* 43, no. 1 (2020): 417-439.  
<https://doi.org/10.1146/annurev-neuro-100219-122527>.
14. Broom, Mark, and Graeme D. Ruxton. 2005. "You can run—or you can hide: optimal strategies for cryptic prey against pursuit predators." *Behavioral Ecology* 16, no. 3: 534-540. <https://doi.org/10.1093/beheco/ari024>.
15. Burns, Fiona, Mark A. Eaton, Ian J. Burfield, Alena Klvaňová, Eva Šilarová, Anna Staneva, and Richard D. Gregory. 2021. "Abundance decline in the avifauna of the European Union reveals cross-continental similarities in biodiversity change." *Ecology and evolution* 11, no. 23: 16647-16660. <https://doi.org/10.1002/ece3.8282>.
16. Brieger, Falko, Jim-Lino Kämmerle, Robert Hagen, and Rudi Suchant. 2022. "Behavioural reactions to oncoming vehicles as a crucial aspect of wildlife-vehicle collision risk in three common wildlife species." *Accident Analysis & Prevention* 168:106564. <https://doi.org/10.1016/j.aap.2021.106564>.
17. Caro, Timothy M. 2005. *Antipredator defenses in birds and mammals*. Chicago: University of Chicago Press.
18. Chan, Alvin Aaden Yim-Hol, Paulina Giraldo-Perez, Sonja Smith, and Daniel T. Blumstein. 2010. "Anthropogenic noise affects risk assessment and attention: the

distracted prey hypothesis." *Biology letters* 6, no. 4: 458-461.

<https://doi.org/10.1098/rsbl.2009.1081>.

19. Cooper Jr, William E. 2009a. "Flight initiation distance decreases during social activity in lizards (*Sceloporus virgatus*)." *Behavioral Ecology and Sociobiology* 63, no. 12: 1765-1771. <https://doi.org/10.1007/s00265-009-0799-1>.

20. Cooper Jr, William E. 2009. "Fleeing and hiding under simultaneous risks and costs." *Behavioral Ecology* 20, no. 3: 665-671. <https://doi.org/10.1093/beheco/arp049>.

21. Cooper, William E., and Daniel T. Blumstein, eds. 2015. *Escaping from predators: an integrative view of escape decisions*. Cambridge: Cambridge University Press.

22. Corcoran, Aaron J., and William E. Conner. 2016. "How moths escape bats: predicting outcomes of predator–prey interactions." *Journal of Experimental Biology* 219, no. 17: 2704-2715. <https://doi.org/10.1242/jeb.137638>.

23. Corcoran, Evangeline, Megan Winsen, Ashlee Sudholz, and Grant Hamilton. 2021. "Automated detection of wildlife using drones: Synthesis, opportunities and constraints." *Methods in Ecology and Evolution* 12, no. 6: 1103-1114. <https://doi.org/10.1111/2041-210X.13581>

24. Davies, Lee, Yuriy Vagapov, Vic Grout, Stuart Cunningham, & Alecksey Anuchin. 2021. "Review of air traffic management systems for UAV integration into urban airspace." In 2021 28th International Workshop on Electric Drives: Improving Reliability of Electric Drives (pp. 1-6). Institute of Electrical and Electronics Engineers. Moscow. Jan 27-29. <https://doi.org/10.1109/IWED52055.2021.9376343>.

25. DeVault, Travis L., Bradley F. Blackwell, Thomas W. Seamans, Michael J. Begier, Jason D. Kougher, Jenny E. Washburn, Phyllis R. Miller, and Richard A. Dolbeer. 2018. "Estimating interspecific economic risk of bird strikes with aircraft." *Wildlife Society Bulletin* 42, no. 1: 94-101. <https://doi.org/10.1002/wsb.859>.
26. DeVault, Travis L., Bradley F. Blackwell, Thomas W. Seamans, Steven L. Lima, and Esteban Fernández-Juricic. 2015. "Speed kills: ineffective avian escape responses to oncoming vehicles." *Proceedings of the Royal Society B: Biological Sciences* 282, no. 1801: 20142188. <https://doi.org/10.1098/rspb.2014.2188>.
27. Dill, L. M. 1974. "The escape response of the zebra danio (*Brachydanio rerio*) I. The stimulus for escape." *Animal Behaviour* 22(3), 711-722. [https://doi.org/10.1016/S0003-3472\(74\)80022-9](https://doi.org/10.1016/S0003-3472(74)80022-9).
28. Dolbeer, Richard A. 2011. "Increasing trend of damaging bird strikes with aircraft outside the airport boundary: implications for mitigation measures." *Human-Wildlife Interactions* 5, no. 2 :235-248. <https://www.jstor.org/stable/24868885>
29. Dolbeer, Richard A., Michael J. Begier, Phyllis R. Miller, John R. Weller, and Amy L. Anderson. 2023. "Wildlife strikes to civil aircraft in the United States, 1990–2022." *Federal aviation administration national wildlife strike database serial report. Washington (DC): Report of the Associate Administrator of Airports, Office of Safety and Standards, Airport Safety & Certification.* [https://www.faa.gov/airports/airport\\_safety/wildlife/wildlife\\_strikes\\_civil\\_aircraft\\_united\\_states\\_1990\\_2022](https://www.faa.gov/airports/airport_safety/wildlife/wildlife_strikes_civil_aircraft_united_states_1990_2022).

30. Dolbeer, Richard A., John L. Seubert, and Michael J. Begier. 2014. "Population trends of resident and migratory Canada geese in relation to strikes with civil aircraft." *Human-Wildlife Interactions* 8, no. 1: 88-99. <https://www.jstor.org/stable/24874889>.
31. Domenici, Paolo. 2002. "The visually mediated escape response in fish: predicting prey responsiveness and the locomotor behaviour of predators and prey." *Marine and Freshwater Behaviour and Physiology* 35, no. 1-2: 87-110. <https://doi.org/10.1080/10236240290025635>.
32. Domenici, Paolo, Jonathan M. Blagburn, and Jonathan P. Bacon. 2011a. "Animal escapology I: theoretical issues and emerging trends in escape trajectories." *Journal of Experimental Biology* 214, no. 15: 2463-2473. <https://doi.org/10.1242/jeb.029652>.
33. Domenici, Paolo, Jonathan M. Blagburn, and Jonathan P. Bacon. 2011b. "Animal escapology II: escape trajectory case studies." *Journal of Experimental biology* 214, no. 15: 2474-2494. <https://doi.org/10.1242/jeb.053801>
34. Domenici, Paolo, and Robert W. Blake. 1991. "The kinematics and performance of the escape response in the angelfish (*Pterophyllum eimekei*)." *Journal of Experimental Biology* 156, no. 1: 187-205. <https://doi.org/10.1242/jeb.156.1.187>
35. Domenici, Paolo, and Robert W. Blake. 1993. "Escape trajectories in angelfish (*Pterophyllum eimekei*)." *Journal of Experimental Biology* 177, no.: 253-272. <https://doi.org/10.1242/jeb.177.1.253>
36. Doppler, Megan S., Bradley F. Blackwell, Travis L. DeVault, and Esteban Fernández-Juricic. 2015. "Cowbird responses to aircraft with lights tuned to their eyes: Implications

for bird–aircraft collisions." *The Condor: Ornithological Applications* 117, no. 2: 165-177. <https://doi.org/10.1650/CONDOR-14-157.1>

37. Evans, Dominic A., A. Vanessa Stempel, Ruben Vale, and Tiago Branco. 2019. "Cognitive control of escape behaviour." *Trends in cognitive sciences* 23, no. 4: 334-348. <https://doi.org/10.1016/j.tics.2019.01.012>

38. *Federal Aviation Administration Wildlife Strike Database*. 2024. Federal Aviation Administration, United States Department of Transportation. Accessed on February 12<sup>th</sup>, 2025

39. *Federal Aviation Administration Aerospace Forecasts Fiscal Years 2024–2044*. 2024. Federal Aviation Administration, United States Department of Transportation, 11-38.

40. *Instrument Procedures Handbook: FAA-H-8083-16A*. 2017. Federal Aviation Administration, United States Department of Transportation. New York City: Skyhorse Publishing.

41. Goller, Benjamin, Bradley F. Blackwell, Travis L. DeVault, Patrice E. Baumhardt, and Esteban Fernández-Juricic. 2018. "Assessing bird avoidance of high-contrast lights using a choice test approach: implications for reducing human-induced avian mortality." *Peer J* 6: e5404. <https://doi.org/10.7717/peerj.5404>.

42. Guenin, Shane, Carson J. Pakula, Jonathon Skaggs, Esteban Fernández-Juricic, and Travis L. DeVault. 2024. "Inefficacy of mallard flight responses to approaching vehicles." *PeerJ* 12: e18124. <https://doi.org/10.7717/peerj.18124>.

43. Hammer, Tracey L., Pierre Bize, Benoit Gineste, Jean-Patrice Robin, René Groscolas, and Vincent A. Viblanc. 2025. "Life history stage effects on alert and flight initiation

distances in king penguins (*Aptenodytes patagonicus*).\" *Behavioural processes* 226:  
105166. <https://doi.org/10.1016/j.beproc.2025.105166>

44. Holmes, Tamara L., Richard L. Knight, Libby Stegall, and Gerald R. Craig. 1993.

"Responses of wintering grassland raptors to human disturbance.\" *Wildlife Society  
Bulletin (1973-2006)* 21, no. 4: 461-468. <http://www.jstor.org/stable/3783420>

45. Howland, Howard C. 1974. "Optimal strategies for predator avoidance: the relative  
importance of speed and manoeuvrability.\" *Journal of theoretical Biology* 47, no. 2: 333-  
350. [https://doi.org/10.1016/0022-5193\(74\)90202-1](https://doi.org/10.1016/0022-5193(74)90202-1)

46. Huijser, Marcel P., Christa Mosler-Berger, Mattias Olsson, and Martin Strein. 2015.

"Wildlife warning signs and animal detection systems aimed at reducing wildlife-vehicle  
collisions.\" *Handbook of road ecology*: 198-212.

<https://doi.org/10.1002/9781118568170.ch24>

47. Javůrková, V., Šizling, A. L., Kreisinger, J., & Albrecht, T. (2012). An alternative  
theoretical approach to escape decision-making: the role of visual cues. *PloS one*, 7(3),  
e32522.

48. Jun, L. I. U., Yulong, L. I., Xiancheng, Y. U., Xiaosheng, G. A. O., & Zongxing, L. I. U.  
(2018). Design of aircraft structures against threat of bird strikes. *Chinese Journal of  
Aeronautics*, 31(7), 1535-1558.

49. Kawabata, Yuuki, Hideyuki Akada, Ken-ichiro Shimatani, Gregory Naoki Nishihara,  
Hibiki Kimura, Nozomi Nishiumi, and Paolo Domenici. 2023. "Multiple preferred escape  
trajectories are explained by a geometric model incorporating prey's turn and predator  
attack endpoint.\" *Elife* 12: e77699. <https://doi.org/10.7554/eLife.77699>.

50. Kimura, Hibiki, and Yuuki Kawabata. 2018. "Effect of initial body orientation on escape probability of prey fish escaping from predators." *Biology open* 7, no. 7: bio023812. <https://doi.org/10.1242/bio.023812>
51. Lima, Steven L., Bradley F. Blackwell, Travis L. DeVault, and Esteban Fernández-Juricic. 2015. "Animal reactions to oncoming vehicles: a conceptual review." *Biological Reviews* 90, no. 1: 60-76. <https://doi.org/10.1111/brv.12093>.
52. Lind, Johan, Ulrika Kaby, and Sven Jakobsson. 2002. "Split-second escape decisions in blue tits (*Parus caeruleus*)." *Naturwissenschaften* 89, no. 9: 420-423. <https://doi.org/10.1007/s00114-002-0345-8>
53. Liu, Jun, Dudu Zhong, Yulong Li, Zhongbin Tang, Xiaosheng Gao, Zhixue Zhang, and Fuzheng Huang. 2019. "Numerical simulation and test on damage of rotary engine blades impacted by bird." *International journal of crashworthiness* 24, no. 1: 106-120. <https://doi.org/10.1080/13588265.2018.1452548>
54. Lees, Alexander C., Lucy Haskell, Tris Allinson, Simeon B. Bezeng, Ian J. Burfield, Luis Miguel Renjifo, Kenneth V. Rosenberg, Ashwin Viswanathan, and Stuart H.M. Butchart. 2022. "State of the world's birds." *Annual Review of Environment and Resources* 47, no. 1: 231-260. <https://doi.org/10.1146/annurev-environ-112420-014642>.
55. Lunn, Ryan, Patrice E. Baumhardt, Bradley F. Blackwell, Jean Paul Freyssinier, and Esteban Fernández-Juricic. 2023. "Light wavelength and pulsing frequency affect avoidance responses of Canada geese." *PeerJ* 11: e16379. <https://doi.org/10.7717/peerj.16379>.



56. Lunn, Ryan B., Bradley F. Blackwell, Travis L. DeVault, and Esteban Fernández-Juricic. 2022. "Can we use antipredator behavior theory to predict wildlife responses to high-speed vehicles?." *Plos one* 17, no. 5: e0267774.  
<https://doi.org/10.1371/journal.pone.0267774>.
57. Mulero-Pázmány, Margarita., Susanne Jenni-Eiermann, Nicolas Strebel, Thomas Sattler, Juan José Negro, and Zulima Tablado. 2017. "Unmanned aircraft systems as a new source of disturbance for wildlife: A systematic review" *Plos One*, **12(6)**, e0178448.  
<https://doi.org/10.1371/journal.pone.0178448>.
58. Nandutu, Irene, Marcellin Atemkeng, and Patrice Okouma. 2022. "Intelligent systems using sensors and/or machine learning to mitigate wildlife–vehicle collisions: A review, challenges, and new perspectives." *Sensors* 22, no. 7: 2478.  
<https://doi.org/10.3390/s22072478>.
59. Pakula, Carson J., Shane Guenin, Jonathon Skaggs, Olin E. Rhodes Jr, and Travis L. DeVault. 2023. "Driving in the dark: deciphering nighttime driver detection of free-ranging roadside wildlife." *Transportation research part D: transport and environment* 122: 103873.
60. Peterson, Ashley N., Alberto P. Soto, and Matthew J. McHenry. 2021. "Pursuit and evasion strategies in the predator–prey interactions of fishes." *Integrative and comparative biology* 61, no. 2: 668-680.
61. Pfeiffer, Morgan B., Joshua L. Hoblet, Bradley F. Blackwell, and Esteban Fernández-Juricic. 2025. "Preliminary effects of UAS angle of approach on escape responses of a large-bodied raptor." *Drone Systems and Applications* 13: 1-9.  
<https://doi.org/10.1139/dsa-2024-0047>

62. Poot, Hanneke, Bruno J. Ens, Han de Vries, Maurice AH Donners, Marcel R. Wernand, and Joop M. Marquenie. 2008. "Green light for nocturnally migrating birds." *Ecology and Society* 13, no. 2. <https://www.jstor.org/stable/26267982>.
63. Provini, Pauline, Bret W. Tobalske, Kristen E. Crandell, and Anick Abourachid. 2012. "Transition from leg to wing forces during take-off in birds." *Journal of Experimental Biology* 215, no. 23: 4115-4124. <https://doi.org/10.1242/jeb.074484>
64. Rodríguez, Airam, Peter Dann, and André Chiaradia. 2017. "Reducing light-induced mortality of seabirds: high pressure sodium lights decrease the fatal attraction of shearwaters." *Journal for Nature Conservation* 39: 68-72. <https://doi.org/10.1016/j.jnc.2017.07.001>
65. Rosenberg, Kenneth V., Adriaan M. Dokter, Peter J. Blancher, John R. Sauer, Adam C. Smith, Paul A. Smith, Jessica C. Stanton et al. 2019. "Decline of the North American avifauna." *Science* 366, no. 6461: 120-124. <https://doi.org/10.1126/science.aaw1313>.
66. Ruxton, Graeme D., William L. Allen, Thomas N. Sherratt, and Michael P. Speed. 2019. *Avoiding attack: the evolutionary ecology of crypsis, aposematism, and mimicry*. Oxford: Oxford university press.
67. Stankowich, Theodore, and Daniel T. Blumstein. 2005. "Fear in animals: a meta-analysis and review of risk assessment." *Proceedings of the Royal Society B: Biological Sciences* 272, no. 1581 (2005): 2627-2634. <https://doi.org/10.1098/rspb.2005.3251>
68. Van Doren, Benjamin M., David E. Willard, Mary Hennen, Kyle G. Horton, Erica F. Stuber, Daniel Sheldon, Ashwin H. Sivakumar, Julia Wang, Andrew Farnsworth, and Benjamin M. Winger. 2021. "Drivers of fatal bird collisions in an urban

center." *Proceedings of the National Academy of Sciences* 118, no. 24: e2101666118.

<https://doi.org/10.1073/pnas.2101666118>

69. Ventura, Stefânia PR, Conrado AB Galdino, and Paulo Enrique C. Peixoto. "Fatal attraction: territorial males of a neotropical lizard increase predation risk when females are sexually receptive." *Behavioral Ecology and Sociobiology* 75, no. 12 (2021): 170.

<https://doi.org/10.1007/s00265-021-03112-2>

70. Walker, Jeffery A., Cameron K. Ghalambor, O. L. Griscti, D. McKenney, and David N. Reznick. 2005. "Do faster starts increase the probability of evading predators?." *Functional Ecology* 19, no. 5: 808-815. [https://doi.org/10.1111/j.1365-](https://doi.org/10.1111/j.1365-2435.2005.01033.x)

[2435.2005.01033.x](https://doi.org/10.1111/j.1365-2435.2005.01033.x)

71. Wege, Michael L., and Dennis G. Raveling. 1984. "Flight speed and directional responses to wind by migrating Canada Geese." *The Auk* 101, no. 2: 342-348.

<https://doi.org/10.1093/auk/101.2.342>

72. Wickham, Hadley, Winston Chang, and Maintainer Hadley Wickham. 2016. "Package 'ggplot2'." *Create elegant data visualisations using the grammar of graphics. Version 2*, no. 1: 1-189.

73. Ydenberg, Ron C., and Lawrence M. Dill. "The economics of fleeing from predators." In *Advances in the Study of Behavior*, vol. 16, pp. 229-249. Academic Press, 1986.

[https://doi.org/10.1016/S0065-3454\(08\)60192-8](https://doi.org/10.1016/S0065-3454(08)60192-8)

Figure legends

Figure 1. A top-down (a) and front-view (b) illustration of the variables considered in both phase 1 and 2 of the model. All definitions are provided in table 1.

Figure 2. a) The schematic of a Boeing 737 aircraft used to estimate the frontal surface area. The red, dotted line represents the x-axis intercepts of both  $coord_1$  and  $coord_2$  that define the location of the collision window on the x-axis. b) The sum of all pixels per the entirety of the goose body length and relative to each potential location of the goose along the x-axis of the aircraft's trajectory. Here, the right side shows the decrease in the probability of collision as the gooses body length exits the trajectory.

792

793 Figure 3. The relationship between each variable manipulated in our modeling and the  
794 probability of collision, where grey bars represent the standard deviation. a) The mean and  
795 standard deviation in the probability of collision for each of the three light scenarios, where each  
796 point represents the average probability of collision for over 500 runs of the model and with the  
797 same combination of manipulated variables. b) The relation between escape speed (m/s) and  
798 probability of collision for the three light scenarios. c) The relation between sensory-motor  
799 delay (sec) and probability of collision for the three light scenarios. d) The relation between  
800 aircraft approach speed (m/s) and probability of collision for the three light scenarios. e) The  
801 relation between the minimum distance to safety (m) and probability of collision for the three  
802 light scenarios. f) The relation between the minimum distance to safety (m) and probability of  
803 collision for the three light scenarios.

804

805 Figure 4. a) Plot of the average probability of collision for all model predictions made with  
806 a specific flight-initiation distance (m) separated by the three light scenarios. b) Plot of the  
807 average probability of collision for all model predictions made with a specific escape angle  
808 (degree), separated by the three light scenarios.

809

810 Figure 5. a) The relationship between approach speed and the model-predicted probability of  
811 collision compared to the empirical relationship between observed probability of collision and  
812 vehicle approach speed reported in DeVault et al., (2015) & Guenin et al. (2024. b & c). A  
813 density map of the collision locations reported in the FAA wildlife strike database between

814 Canada geese and a 737 aircraft, where b) is the frontal view of an aircraft & c) a top-down view  
815 of the aircraft.

816

817

818

819

820

821

822 Table 1. A list of all variables, their corresponding symbols, definitions and units used for  
823 equations 1 to 6 in the main text.  
824

<u>Symbol</u>	<u>Definition</u>	<u>Units</u>
$T_a$	Time needed for the animal to escape the vehicles trajectory	sec
$T_v$	Time until the vehicle reaches the location of the animal within its trajectory	sec
$D_{min}$	Distance needed to clear the trajectory of the approaching vehicle	m
$l$	Body length or wingspan of the animal	m
$D_{safe}$	The total distance the animal needs to travel to reach safety (Eq.1)	m
$S_a$	Escape speed of the animal	m/s
$\theta$	Escape angle ranging from 0 to 180 degrees, where 0 is directly towards the approaching vehicle and 180 degrees is directly away	deg
$\delta$	The time needed for the animal to re-orient and initiate escape	sec
$D_{FID}$	Flight-initiation distance or distance between the animal and the aircraft when the animal initiates escape	m
$S_v$	Approach speed of vehicle	m/s
$D_{height}$	The maximum height of the approaching vehicle	m

$D_{width}$	The maximum width of the approaching vehicle	m
$D_{initial}$	The animal's initial position within the vehicle's trajectory relative vehicle width (Eq. 4)	m
$D_{collision}$	The animal's position within the vehicle's trajectory relative to vehicle width when the vehicle reaches the location of the animal (Eq. 5)	m
$A_{front}$	The frontal surface area of the approaching aircraft	m <sup>2</sup>

825

826

827

828

829

830

831

832

833

834

835

836

837

838

839



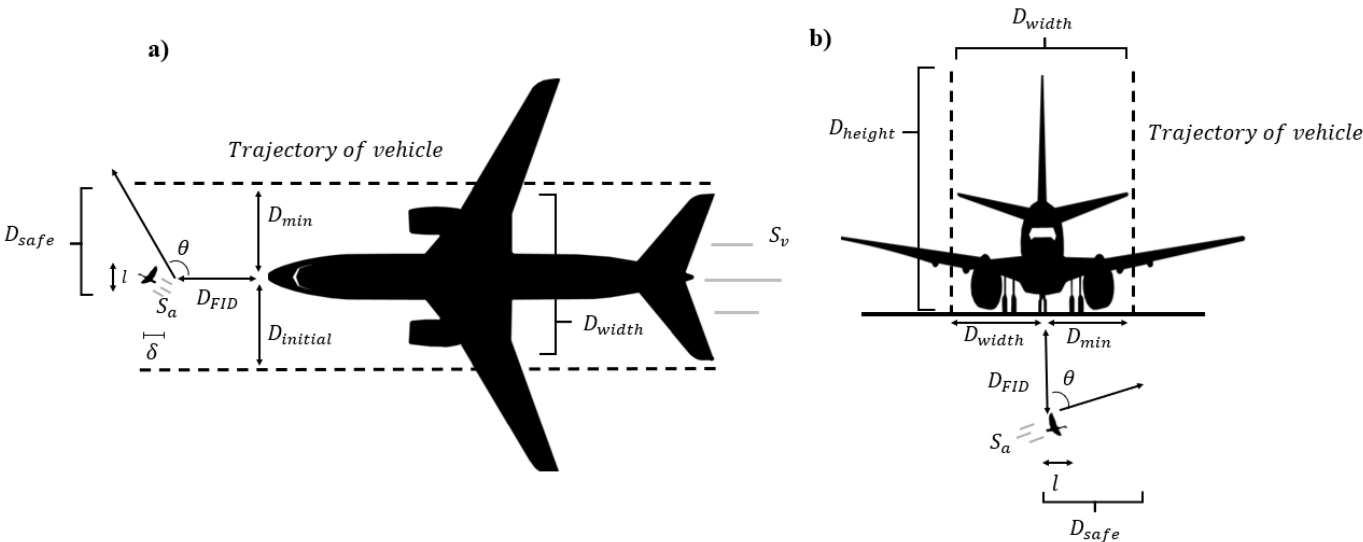
840 Table 2. A list of the model assumptions  
841

Assumptions	
1	The vehicle is approaching directly, alternatively the animal is within the path trajectory of the vehicle.
2a	The trajectory of the vehicle is linear and constant
2b	Vehicle approach speed ( $S_v$ ) is constant
3a	The trajectory of the animal is linear and constant after it initiates escape
3b	Animal escape speed is constant ( $S_a$ ) after it initiates escape
4	The animal can be located at any altitude within the trajectory of the vehicle
5	Per the light application exercise, towards escape angles are paired with shorter flight-initiation distances as part of a larger attraction response to the light stimuli

842

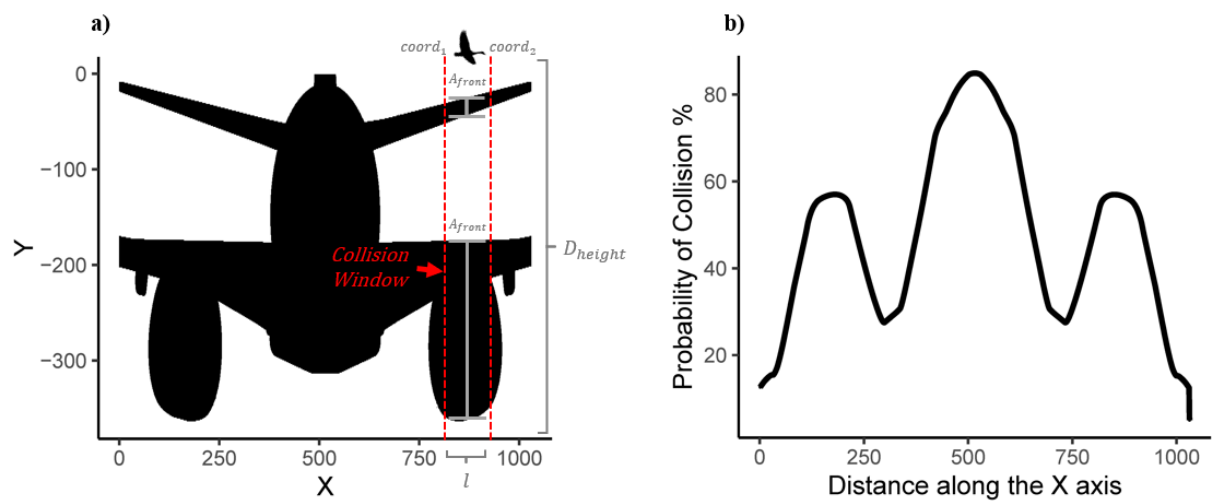
843

844     Figure 1.



845  
846  
847  
848  
849  
850  
851  
852  
853  
854  
855  
856  
857  
858  
859  
860  
861  
862  
863  
864  
865  
866  
867  
868  
869

870 Figure. 2



871  
872  
873  
874  
875  
876  
877  
878  
879  
880  
881  
882  
883  
884  
885  
886  
887  
888  
889  
890  
891  
892  
893  
894  
895  
896  
897  
898  
899  
900

Figure 3.

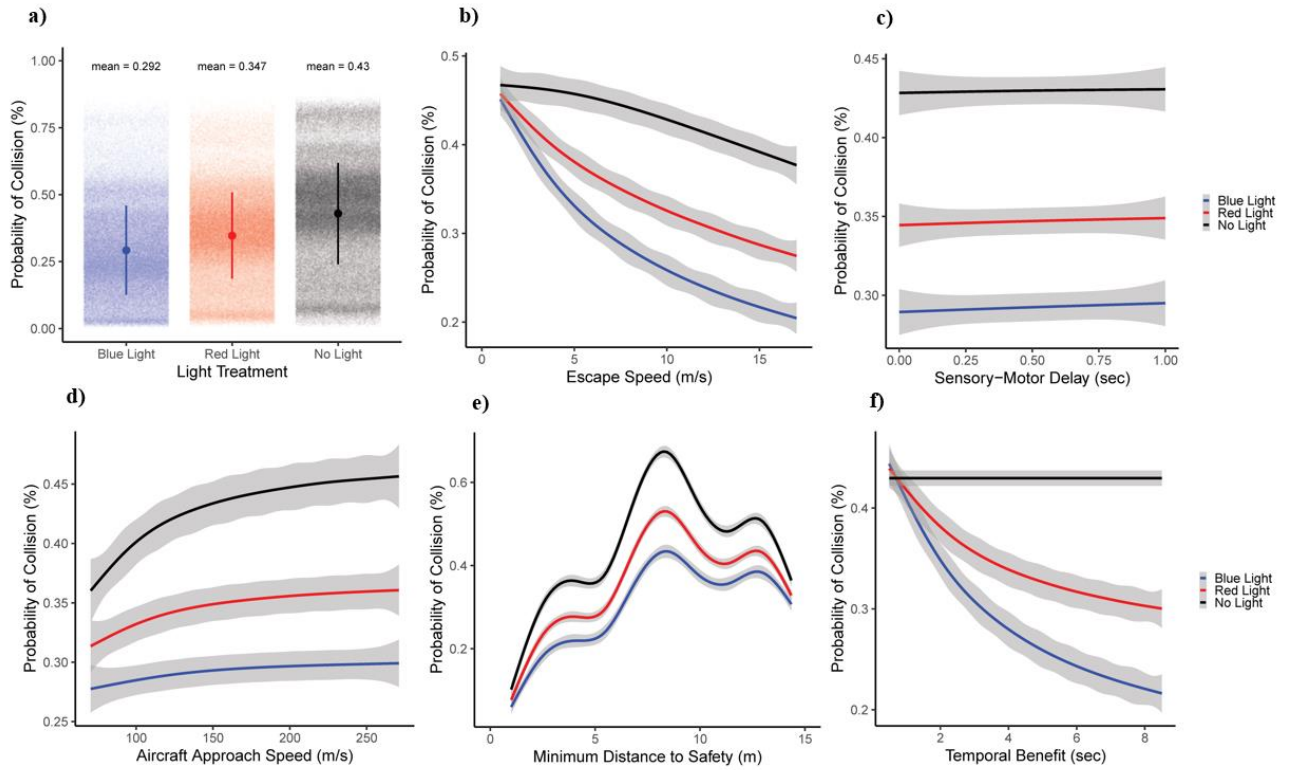


Figure 4.

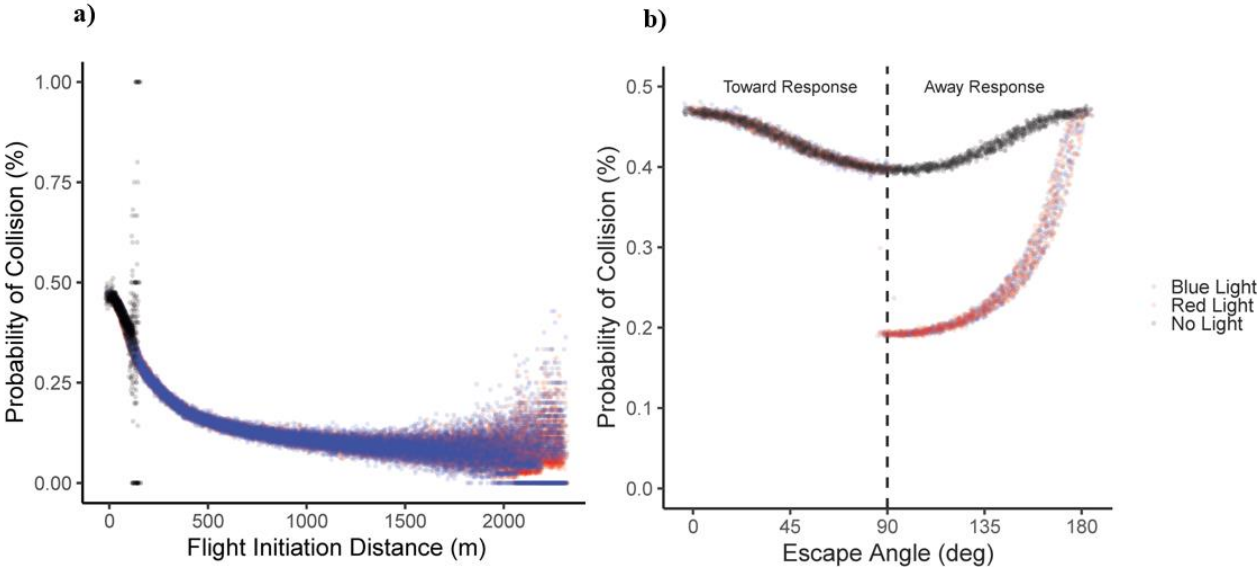
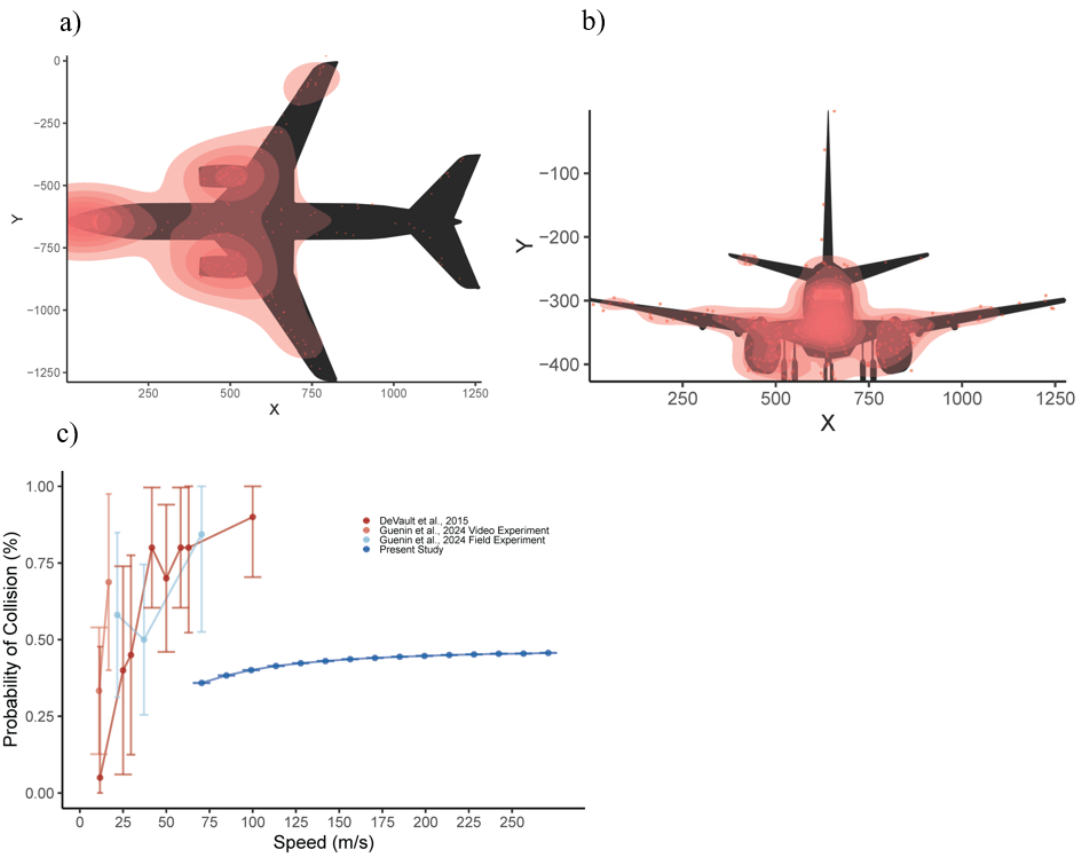


Figure 5.



953  
954  
955  
956  
957  
958

959

960

961

962

963

964

965

966